Association of Ice and River Channel Morphology Determined Using Ground-penetrating Radar in the Kuparuk River, Alaska

Authors: Best, Heather, McNamara, James P., and Liberty, Lee

Source: Arctic, Antarctic, and Alpine Research, 37(2) : 157-162

Published By: Institute of Arctic and Alpine Research (INSTAAR), University of Colorado

URL: https://doi.org/10.1657/1523-0430(2005)037[0157:AOIARC]2.0.CO;2

Arctic, Antarctic, and Alpine Research, Vol. 37, No. 2, 2005, pp. 157–162

Association of Ice and River Channel Morphology Determined Using Ground-penetrating Radar in the Kuparuk River, Alaska

*Heather Best**
James P. McNamara‡ and*
Lee Liberty†

*Department of Geosciences,
Boise State University, Boise,
ID 83725, U.S.A.
†Center for Geophysical Investigation of
the Shallow Subsurface,
Boise State University, Boise,
ID 83725, U.S.A.
‡Corresponding author.
JMCNAMAR@boisestate.edu

Abstract

We collected ground-penetrating radar data at 10 sites along the Kuparuk River and its main tributary, the Toolik River, to detect unfrozen water beneath river ice. We used 250 MHz and 500 MHz antennas to image both the ice-water interface and the river channel in late April 2001, when daily high temperatures were consistently below freezing and river ice had attained its maximum seasonal thickness. The presence of water below the river ice appears as a strong, horizontal reflection observed in the radar data and is confirmed by drill hole data. A downstream transition occurs from ice that is frozen to the bed, called bedfast ice, to ice that is floating on unfrozen water, called floating ice. This transition in ice type corresponds to a downstream change in channel size that was detected in previously conducted hydraulic geometry surveys of the Kuparuk River. We propose a conceptual model wherein the downstream transition from bedfast ice to floating ice is responsible for an observed step change in channel size due to enhanced bank erosion in large channels by floating ice.

Introduction

The shape of a river channel is a product of the relationship between climate and physical properties of the landscape. In arctic regions it is therefore likely that ice and permafrost, two dominant properties of the arctic landscape, exert important controls on fluvial form. McNamara (2000) reported an anomalous property in the downstream hydraulic geometry of the Kuparuk River in northern Alaska, U.S.A., wherein a step-change exists in the log-linear relationship between channel cross-sectional area and drainage area (Fig. 1). That study suggested that the anomaly may be related to downstream changes in ice conditions and consequent changes in erosion processes based on the observation that, at one headwater site, the river freezes to the stream bed every winter, here called bedfast ice, whereas near the mouth of the river there is typically water in the bottom of the channel under a cap of ice, here called floating ice. Where bedfast ice is present, the spring snowmelt water flows over ice for most of the duration of the melt period. The bed sediments are therefore protected and sediment transport is limited (Oatley, 2002). Where floating ice is present, the snowmelt water carries the ice downstream and the sediment is available for transport. Furthermore, floating ice may enhance erosion by scouring the banks (Smith, 1979; Walker and Hudson, 2003). McNamara (2000), however, presented limited data to support the ice transition/channel morphology hypothesis.

In this study we take a first step to test this hypothesis—namely, to determine if the hydraulic geometry anomaly illustrated in Figure 1 corresponds to a downstream transition from bedfast ice to floating ice in the Kuparuk River basin. We map the occurrence of floating ice and bedfast ice using ground-penetrating radar (GPR), model the potential ice thickness in the river using a degree-day method, and compare the distributions of floating ice and bedfast ice to the hydraulic geometry anomaly.

Study Location

The Kuparuk River flows from the foothills of the Brooks Range northward across tundra to the Beaufort Sea (Fig. 2). The entire region lacks trees, is underlain by continuous permafrost, and is covered with snow for 7 to 9 months each year. Permafrost thickness ranges from around 250 m near the foothills to over 600 m near the coast (Osterkamp and Payne, 1981), which effectively isolates groundwater from surface water (McNamara et al., 1998). The Kuparuk River basin encompasses 8140 km^2, with an average elevation of 245 m. The basin contains no glaciers, but its higher regions have been shaped by past glaciations (Detterman et al., 1958). The flow season typically begins in late May in the headwaters, and in early June near the coast. Freeze-up typically begins in mid-September to early October. The snowmelt flood is consistently a dominant hydrologic event each year in the lower regions of the watershed, but occasional summer rainstorms produce floods that meet or exceed the snowmelt flood in the headwater regions (Kane et al., 2000, 2003).

Methods

GPR SURVEY

We used GPR to detect ice/water and ice/sediment interfaces at several locations throughout the Kuparuk River basin. GPR transmits short pulses of high frequency EM energy into the ground, generating a wavefront which propagates downward. Due to a change in the bulk electrical properties of different subsurface materials, some of the energy is reflected back to the surface. A receiving antenna monitors reflected energy through time. The strength of the reflected signal is approximately proportional to the difference in dielectric constants at the subsurface discontinuity. If the propagation velocity of the subsurface material is known, we can calculate reflection depths. Further GPR theory and methodology are explained in numerous publications (e.g., Davis and Annan, 1989; Jol and Smith, 1991).

Detecting the interface between water and ice in a river channel is an ideal application for GPR because the bulk electrical properties of the two materials are so disparate; freshwater at 0°C and freshwater ice have dielectric constants of 88 and 3.2, respectively. For example, Delaney et al. (1990) conducted surface and airborne radar surveys on the Tanana River of central Alaska to create ice thickness profiles, Arcone and Delaney (1987) used airborne GPR to map river ice thickness, and Arcone et al. (1992, 1998) used GPR to detect unfrozen

1523-0430/05 $7.00

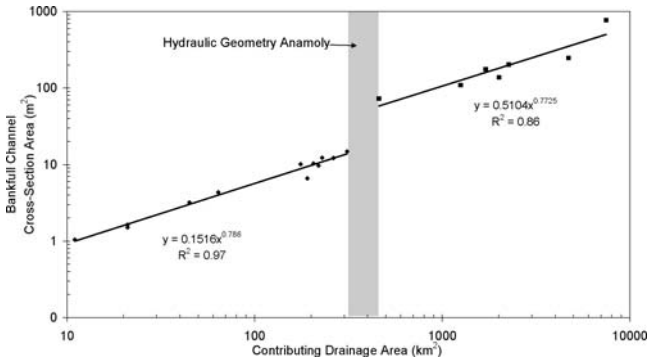

FIGURE 1. Plot of Kuparuk River channel cross-sectional area against drainage area, showing a "jump" in channel size at a threshold drainage area (A_{th} of 300–600 km^2) (fig. modified from McNamara, 2000).

water beneath ice blisters along the Sagavanirktok River, a parallel drainage to the Kuparuk River.

We traveled throughout the basin using a helicopter to conduct the GPR survey during late April 2001, prior to the snowmelt period when the river ice had presumably attained its maximum annual thickness. Locations for the GPR reflection profiles on the Kuparuk River were initially the same as those visited for the hydraulic geometry surveys of McNamara (2000). We acquired several GPR profiles of channel cross-sections and one longitudinal profile linking the cross-sections at each of the 10 selected sites (Fig. 2). Each transect was made on foot with one person carrying the laptop computer and control unit and dragging the antenna housing across the snow on a sled. We initially focused on sites where bedfast ice was likely to appear. We then shifted downstream to locations where floating ice likely appeared and lastly visited sites between, near the ice-type transition zone. In the lower reaches where the river exhibits large meanders, we acquired profiles at river bends to image the deeper sections of the channel.

We used Malå Geoscience Corporation GPR hardware and software. The control unit was a Malå/RAMAC CU2 model. The transmitter and receiver antennas operated near 250 MHz and 500 MHz center frequencies and were contained in shielded housings. The shielded antenna system minimized interference from objects on the surface (i.e., GPR-related hardware, snowshoes, and other communications-related energy sources). The antenna separations were fixed at 18 cm for the 500 MHz and 36 cm for the 250 MHz antennas. The two different antenna frequencies were independently deployed to best image targets at various depths. A hip-chain and string attached to a fixed point triggered the control unit to record an energy pulse at

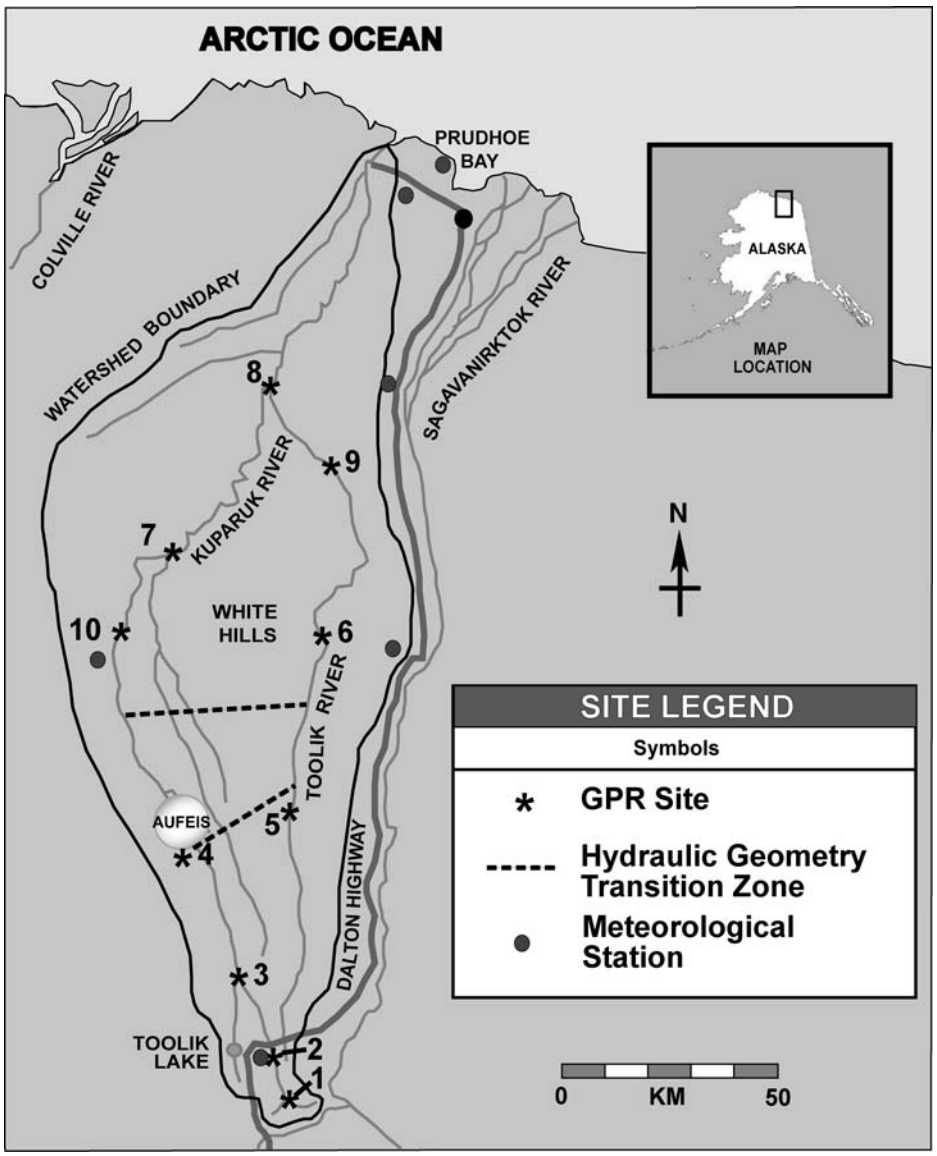

FIGURE 2. Physiographic map showing the Kuparuk basin on the North Slope of Alaska, meteorological stations, and our GPR survey locations.

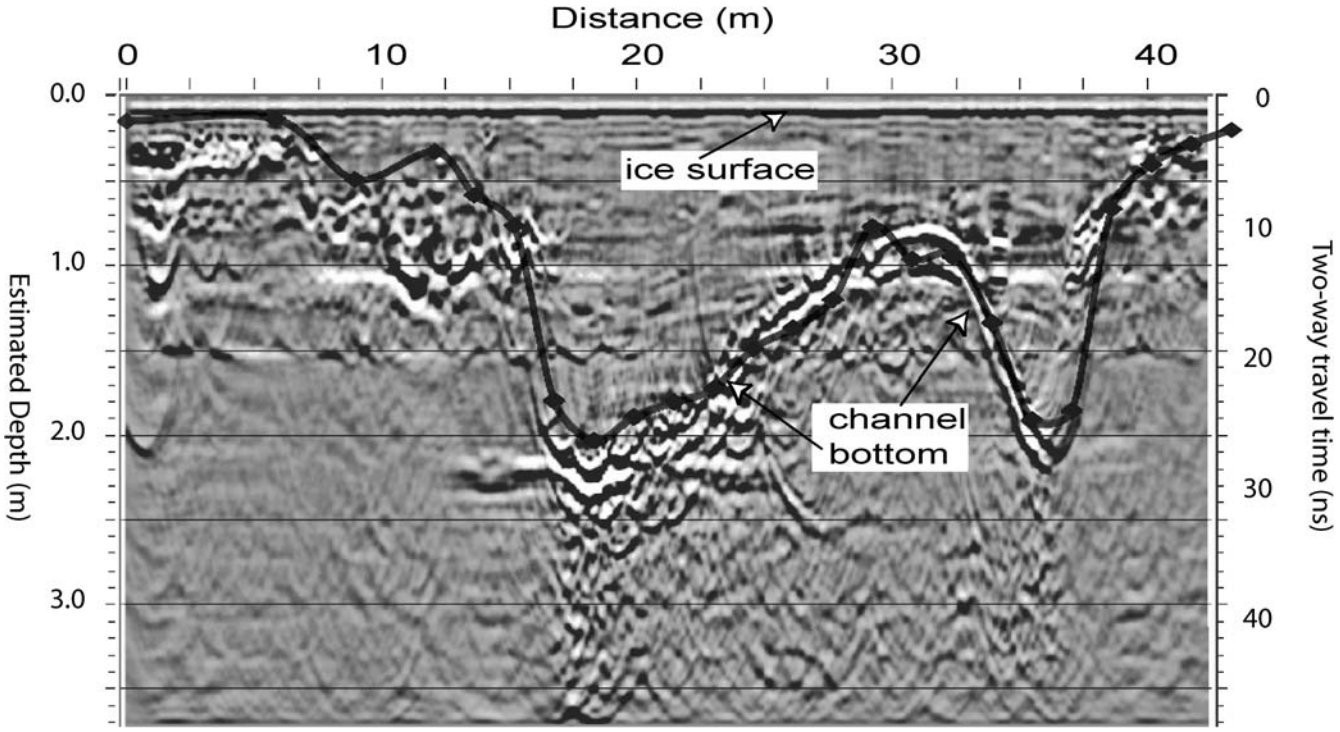

FIGURE 3. A 500 MHz GPR migrated reflection profile from Site 2 showing the presence of bedfast ice. Note the distinct channel margins of the signal from the ice surface. There is no reflection within the channel that would suggest the presence of water within the channel. Estimated depths

10-cm intervals. We collected 8 stacks per sampling location for the 500 MHz antennas and 4 stacks per sampling location for the 250 MHz antennas. A laptop computer, hosting Malå/RAMAC GroundVision software, recorded and displayed the received traces.

After completion of the surveys, we performed additional processing steps to enhance the ice-water interface and channel margins. We applied a low pass filter to remove low-frequency noise caused by electronic antenna overload (e.g., Daniels et al., 1988), eigenvector filters to attenuate coherent noise, migration to place reflections in their proper spatial position, and automatic gain control (AGC) to counter signal attenuation with depth and to improve the display of our results.

We identified ice/water and ice/sediment interfaces by visual inspection of the GPR velocity profiles. We display our GPR profiles with two-way traveltime of radar energy on the right vertical axis and distance on the horizontal axis (Figs. 3 and 4). Depth on the left vertical axis is estimated by converting the traveltime to distance for the observed reflection using the velocity of radar waves in freshwater ice (0.168 m/ns) and water (0.03 m/ns). We used the higher resolution 500 MHz antennas to identify ice/water reflection to calculate ice thickness. The GPR ice thickness estimation was checked by augering through the ice at two locations.

POTENTIAL ICE THICKNESS MODELING

Bedfast ice occurs where the climate-driven potential ice thickness is greater than the depth of the channel, and floating ice occurs where the potential ice thickness is less than the depth of the channel. The Accumulative Freezing Degree-Day (AFDD) equation (U.S. Army Corps of Engineers, 1981) calculates potential ice thickness by assuming that ice thickness is proportional to the square root of the accumulated freezing degree-days,

$$h_n = \alpha\sqrt{\sum_{i=1}^{n} t(T_m - T_s)_i} \quad (1)$$

where h is potential ice thickness (cm) after i days since initial ice formation, n is number of days in the simulation, T_m is the average daily temperature of the bottom ice surface, T_s is the average daily temperature of the top ice surface, t is one day, and α is an empirical coefficient representative of the river type. We assume that T_m is 0°C and T_s equals the local air temperature. Initial formation of ice on the surface of a river is not accounted for in the AFDD equation.

We started the ice thickness calculations ($i = 1$) after 5 consecutive days with below-freezing air temperatures occurring in the fall to allow for initial ice formation and ended the calculations ($i = n$) after 5 consecutive days occurring in the spring with average temperatures above freezing. The arbitrary selection of 5 days has little impact on h_n because of the long freezing season. We solved Equation 1 for each GPR survey location by first calculating degree-days accumulated by 25 April at 5 meteorological stations distributed throughout the watershed (Fig. 2). We established a linear relationship between degree-days and latitude, which was used to calculate degree-days at each GPR survey location. We solved Equation 1 for the coefficient α at each site where floating ice was detected, then used the average α to calculate h_n for all sites.

COMPARING ICE THICKNESS TO HYDRAULIC GEOMETRY

Although the hydraulic geometry anomaly illustrated in Figure 1 is reported using A_{xsec}, a two-dimensional measure, we compare ice type and ice thickness to maximum channel depth, D_{max}, a one-dimensional component of A_{xsec}. We use D_{max} because we assume that if water is present under floating ice it will occur in the deepest part of the channel. D_{max} values were obtained from the hydraulic geometry surveys that were used to derive A_{xsec} in McNamara (2000). We briefly

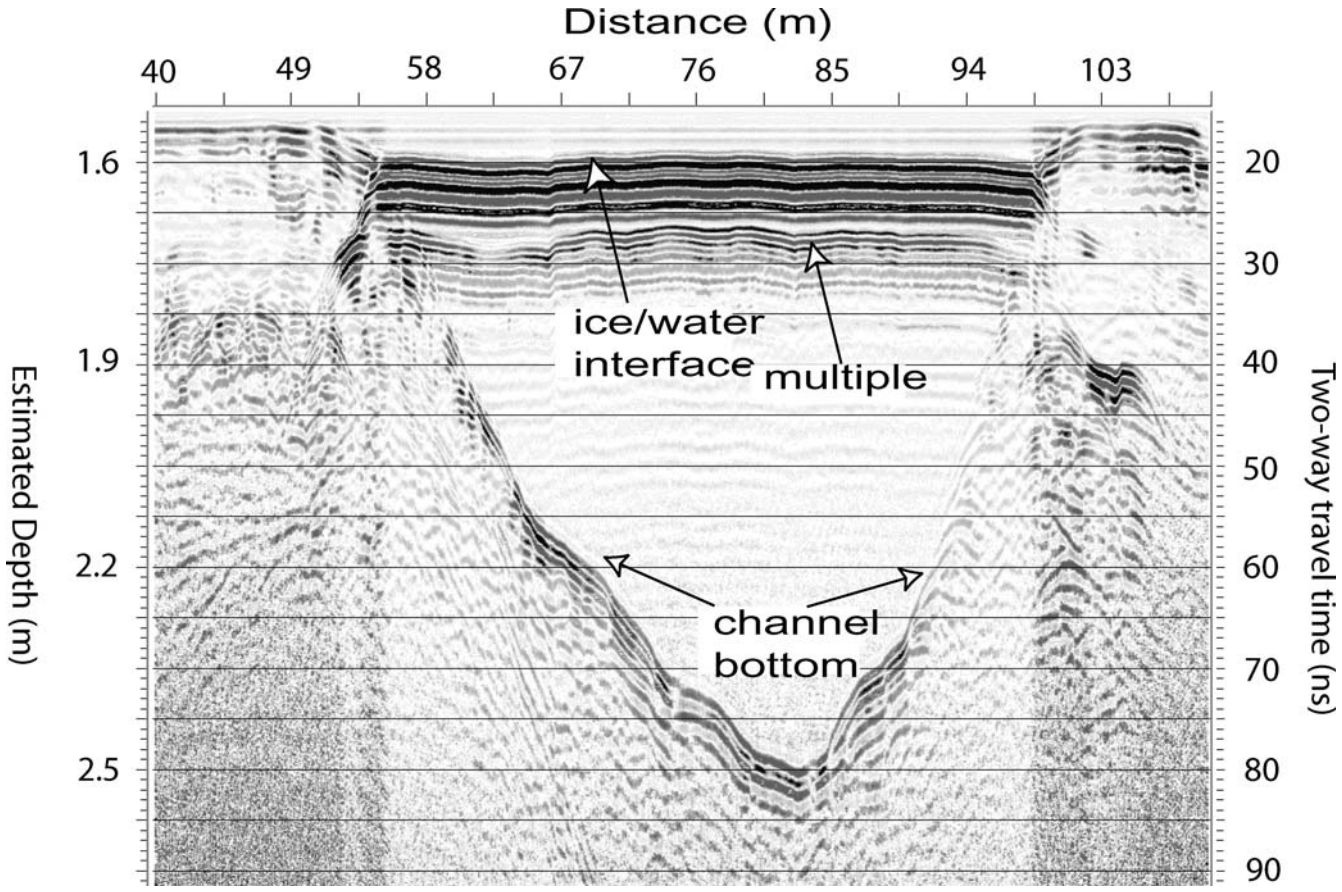

FIGURE 4. A 250 MHz GPR reflection profile from Site 7 showing floating ice at approximately 1.7 m depth, inferred from the presence of a strong horizontal reflection and confirmed by drilling through the ice. Estimated depths are calculated using freshwater ice radar velocities to the ice/water contact and freshwater radar velocities below.

summarize the field methods here. Twenty-one reaches draining areas ranging between 21 km^2 and 7465 km^2 were surveyed in the Kuparuk River basin during a 3-day low-water period in June 1999. At each reach two channel cross-sections and a longitudinal profile were surveyed and the elevations of bankfull stage and other morphologic features were noted. Bankfull stage was identified following the recommendations of Williams (1978), who stated that the best indicator of bankfull stage is a flat, depositional surface adjacent to the river. This surface may be continuous or discontinuous, and may be a narrow strip below a higher terrace or it may be a broad plain. Maximum channel depth is the height of bankfull stage above the lowest elevation in the cross-section.

Results

GPR SURVEY

We classify each field site into two categories, one with the presence of bedfast ice and one with the presence of floating ice. Reflection profiles for Sites 1, 2, 3, 4, 5, and 10 show the presence of bedfast ice (Table 1). Each profile from this category has one distinct reflection that correlates with channel depth and a strong reflection that appears at the snow/ice interface. We imaged the complete channel for most of the bedfast ice sites using the 500 MHz antennas because of the relatively shallow depth of the upstream channel reaches. In a migrated radar image from Site 2, Figure 3 shows a horizontal reflection immediately below the ground surface that correlates with the observed depth of the snow/ice interface. Also, the prominent reflection that varies in depth from 0 to 2 m shows a strong relationship with the measured channel boundary (gray line) and represents the ice/sediment reflection. The complexity of the ice/sediment reflection represents both the observed steep dips present at this site and processing artifacts from the migration process. The processing artifacts are caused by large lateral and vertical radar velocity variations at the ice/sediment boundary. Without the migration process, the correlation between the reflection shape and the measured channel boundary are reduced. We confirmed that no water was present at Site 2 by drilling through the ice to the channel bottom.

Reflection profiles for Sites 6, 7, 8, and 9 (Fig. 2) show the presence of floating ice (Table 1). A strong horizontal reflection from the boundary between ice and water is present in each profile. An example from Site 7 is presented in Figure 4. We chose to minimize the processing on Figure 4 to show the clear identification of the ice/water and water/channel reflections on field data. The characteristic ringing signal caused by reflection multiples follows the ice/water interface due to the strong contrasts in dielectric properties across this boundary. The other prominent reflection appears at the water/sediment interface and correlates with the channel margin. The boundaries of this unmigrated image (Fig. 4) are slightly misplaced, as seen by the ice surface that crosses the channel margin reflection, but the identification of the ice/water interface is unmistakable.

ICE THICKNESS

Ice thickness determined by GPR for floating ice sites ranged between 151 cm and 176 cm (Table 1). A two-layer model using radar

TABLE 1

Ice thickness calculations at GPR survey locations; n.a. = not applicable.

Site	Latitude (UTM)	Drainage area (km^2)	GPR profiles	Ice/water two-way arrival time (ns)	GPR ice thickness (cm)	Auger ice thickness (cm)	Alpha	Degree-days	Potential ice thickness (cm)			
									$\alpha = 0.77$	$\alpha = 0.4$	$\alpha = 0.6$	$\alpha = 0.9$
1	7609199	45	7	n.a.	Grounded	n.a.	n.a.	44899	162	85	127	191
2	7615156	142	5	n.a.	Grounded	n.a.	n.a.	44940	162	85	127	191
3	7633207	191	5	n.a.	Grounded	n.a.	n.a.	45064	163	85	127	191
4	7656856	206	4	n.a.	Grounded	n.a.	n.a.	45228	163	85	128	191
5	7667069	233	4	n.a.	Grounded	n.a.	n.a.	45298	163	85	128	192
6	7711325	1253	2	21	176	n.a.	0.83	45603	163	85	128	192
7	7728347	2734	8	20	168	172	0.79	45721	164	86	128	192
8	7770904	7465	1	19	160	n.a.	0.74	46014	164	86	129	193
9	7741965	2007	3	18	151	n.a.	0.71	45815	164	86	128	193
10	7704694	1640	1	n.a.	Grounded	n.a.	n.a.	45558	163	85	128	192

velocities in ice and water for Site 7 shows an estimated ice thickness of 168 cm and a maximum channel depth of 258 cm. We augered through the ice at Site 7 and measured a thickness of 172 cm. The maximum channel depth from the hydraulic geometry survey for this site is 270 cm, which is a good comparison with the GPR profile considering that we could not locate the exact position of the hydraulic geometry survey and the elevation of bankfull stage was obscured by ice.

The calculated parameter α ranged between 0.71 and 0.83, with an average and standard deviation of 0.77 and 0.05 (Table 1). The U.S. Army Corps of Engineers (1981) states that α ranges between 0.4 and 0.9, and it is common to assume $\alpha = 0.6$. We calculated potential ice thickness using 0.4, 0.6, 0.77, and 0.9 to present a range of possible solutions. Degree-days did not vary considerably across the watershed, and the resulting potential ice thicknesses were fairly constant with latitude (Table 1, Fig. 5).

The ice thickness estimations using GPR and degree-day modeling are for only 1 year, whereas channel morphology is the product of long-term processes. A t-test performed at the 99% confidence level on data from 3 meteorological stations throughout the Kuparuk River basin shows that cumulative degree-days from winter 2000–2001 are not significantly different than the average for winters from 1990–2000 (Best, 2002), suggesting that our 1-year ice thickness calculations might represent a long-term average.

COMPARISON OF ICE THICKNESS TO CHANNEL DEPTH

We observed bedfast ice at all locations upstream of the hydraulic geometry anomaly, and floating ice at all sites except one (Site 10) downstream of the anomaly (Table 1, Fig. 5). At Site 10 (Fig. 2), logistical constraints forced us to conduct only one cross-sectional survey, whereas we conducted multiple cross-sectional surveys at each of the other sites. Regardless, we do not expect there to be a distinct downstream change from bedfast ice to floating ice, but that there will be a transition zone influence by local controls.

The potential ice thickness calculated using the empirical $\alpha = 0.77$ intersects the channel depth trend downstream of the anomaly (Fig. 5), but falls below the channel depth trend at all but one hydraulic geometry survey location. The potential ice thickness calculated using $\alpha = 0.6$ cleanly separates channel depths upstream and downstream of the hydraulic geometry anomaly. These favorable comparisons support the suggestion posed by McNamara (2000) that there is a correlation between the hydraulic geometry anomaly illustrated in Figure 1 and a downstream transition from bedfast ice to floating ice.

Discussion

Although our results support the hypothesis that the hydraulic geometry anomaly illustrated in Figure 1 corresponds to a downstream

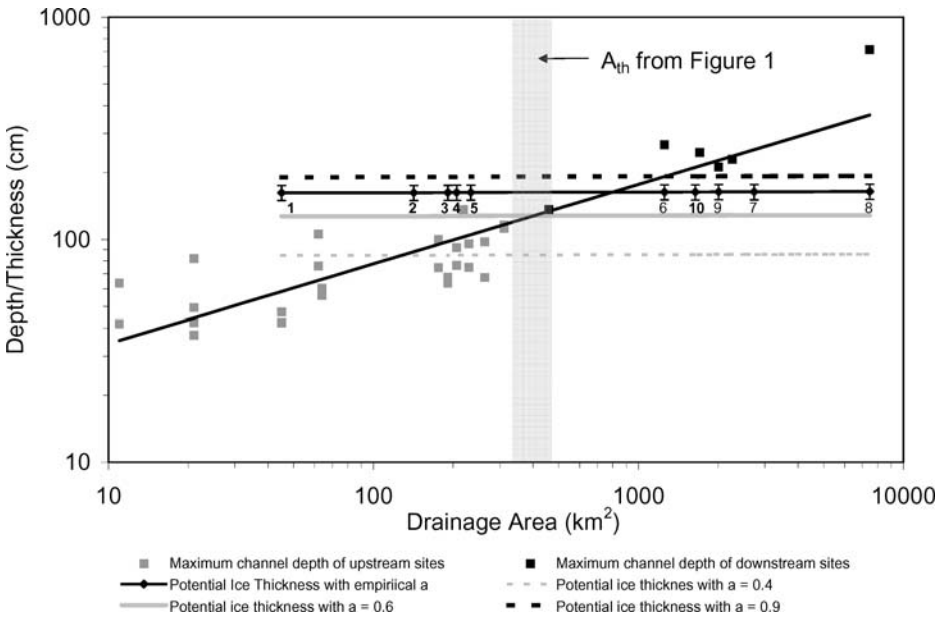

FIGURE 5. Plot showing the relationships between channel depth and potential ice thickness. The numbered symbols on the empirical ice thickness line correspond to GPR survey locations. Bold numbers indicate where bedfast ice was observed. Black and gray squares indicate positions downstream and upstream of the hydraulic geometry transition. The shaded vertical bar corresponds to the hydraulic geometry anomaly from Figure 1. The potential ice thickness lines are calculated using Equation 1 with different α.

transition from bedfast ice to floating ice in the Kuparuk River basin, they do not address the more pressing question of cause and effect. Does the presence of floating ice or bedfast ice control channel morphology, or vice versa? Further, are the upstream channels undersized or are the downstream channels oversized? We propose a conceptual model to explain the co-evolution of channel morphology and the long-term average ice condition. Channels upstream of the hydraulic geometry anomaly form as a result of summer fluvial processes with little influence from the spring snowmelt. Channels increase in size downstream by a power function (Fig. 1) until they become deep enough to support floating ice at the hydraulic geometry anomaly. At this point, the shift in channel size could be accommodated by enhanced erosion during the snowmelt period by the action of ice on the banks, or simply that the bed is no longer protected by bedfast ice. Note, however, that the step-change in A_{xsec} (Fig. 1) does not occur in channel depth (Fig. 5). Because A_{xsec} is the product of channel depth and channel width, the step-change in A_{xcec} is therefore accomplished by a step-change in channel width. This implies that across the hydraulic geometry anomaly, a shift in the dominance of erosion processes occurs that favors channel widening over channel deepening. This supports the suggestion that the shift in channel size occurs by enhanced bank erosion by ice during the snowmelt period.

An alternative model is that ice type is not causing downstream changes in channel morphology, but that another external factor causes downstream changes in channel morphology, which then causes the downstream change in ice type. Such external factors may include changes in channel slope, lithologic changes, or the distribution of icings.

Conclusions

We acquired GPR data at 10 sites in the Kuparuk River basin and, combined with ice thickness models, located a transition zone from bedfast ice to floating ice near the drainage area where a step-increase in channel cross-section area occurs. This spatial association implies that ice type and channel size are related. We propose that the adjustment in channel size is caused by a change in the dominant erosion processes as ice transitions downstream from bedfast to floating. Field measurements on erosion and sediment transport during the snowmelt period are required to validate this idea. Further, future work in other arctic rivers will indicate whether this hydraulic geometry anomaly is a characteristic of all arctic rivers or limited to the Kuparuk.

The relationship between ice and channel morphology has significance for studies concerning the hydrologic response of arctic watersheds to climate change. As the climate warms, we can expect a change in permafrost conditions and in the ice regime of arctic rivers. These changes could potentially lead to a dynamic readjustment of channel morphology and consequent changes in hydrologic response and sediment delivery to the Arctic Ocean.

Acknowledgments

This work was funded by the National Science Foundation, Office of Polar Programs Grant OPP-9814984 in collaboration with Douglas Kane and Larry Hinzman at the Water and Environmental Research Center at the University of Alaska Fairbanks. We thank Steve Arcone and an anonymous reviewer for their insightful comments, which substantially improved the manuscript.

References Cited

Arcone, S. A., and Delaney, A. J., 1987: Airborne river-ice thickness profiling with helicopter-borne UHF short-pulse radar. *Journal of Glaciology,* 33(115): 330–340.

Arcone, S. A., Chacho, E. F., and Delaney, A. J., 1992: Short-pulse radar detection of groundwater in the Sagavanirktok River floodplain in early spring. *Water Resources Research,* 28(11): 2925–2936.

Arcone, S. A., Chacho, E. F., and Delaney, A. J., 1998: Seasonal structure of taliks beneath arctic streams determined with ground-penetrating radar. *Proceedings of the 7th International Permafrost Conference*, Yellowknife, NWT, June 1998, 19–24.

Best, H., 2002: The influence of ice on channel morphology of the Kuparuk River, Alaska. Masters thesis. Boise, Idaho, Boise State University, 76 pp.

Daniels, D. J., Gunton, D. J., and Scott, H. F., 1988: Introduction to subsurface radar. *IEE Proceedings,* 135(4): 278–320.

Davis, J. L., and Annan, A. P., 1989: Ground penetrating radar for high resolution mapping of soil and rock stratigraphy. *Geophysical Prospecting,* 37: 531–551.

Delaney, A. J., Arcone, S. A., and Chacho, E. F., 1990: Winter short-pulse radar studies on the Tanana River, Alaska. *Arctic,* 43(3): 244–250.

Detterman, R. L., Bowsher, A. L., and Dutro, J. T., Jr., 1958: Glaciation on the Arctic Slope of the Brooks Range, northern Alaska. *Arctic,* 11(1): 43–61.

Jol, H. M., and Smith, D. G., 1991: Ground penetrating radar of northern lacustrine deltas. *Canadian Journal of Earth Sciences,* 28: 1939–1947.

Kane, D. L., Hinzman, L. D., McNamara, J. P., Zhang, Z., and Benson, C. S., 2000: An overview of a nested watershed study in Arctic Alaska. *Nordic Hydrology,* 4/5: 245–266.

Kane, D. L., McNamara, J. P., Yang, D., Olson, P. Q., and Gieck, R. E., 2003: An extreme rainfall event in Arctic Alaska. *Journal of Hydrometeorology,* 4(6): 1220–1228.

McNamara, J. P., 2000: Bankfull flow, hydraulic geometry, and river ice in a northern river. *Proceedings: AWRA Water Resources in Extreme Environments*, May 2000, Anchorage, Alaska, 191–196.

McNamara, J. P., Kane, D. L., and Hinzman, L. D., 1998: An analysis of streamflow hydrology in an Arctic drainage basin: A nested watershed approach. *Journal of Hydrology,* 206: 39–57.

Oatley, J. A., 2002: Ice, bedload transport, and channel morphology on the upper Kuparuk River. Master thesis. University of Alaska Fairbanks, 92 pp.

Osterkamp, T. E., and Payne, M. W., 1981: Estimates of permafrost thickness from well logs in northern Alaska. *Cold Regions Science and Technology,* 1: 13–27.

Smith, D. G., 1979: Effects of channel enlargement by river ice processes on bankfull discharge in Alberta, Canada. *Water Resources Research,* 15(2): 469–475.

U.S. Army Corps of Engineers, 1981:*Prediction and calculation of incremental ice thickening*, 6 pp.

Walker, H. J., and Hudson, P. F., 2003: Hydrologic and geomorphic processes in the Colville River delta, Alaska. *Geomorphology,* 56: 291–303.

Williams, G. P., 1978: Bank-full discharge of rivers. *Water Resources Research,* 14(6): 1141–1154.

Revised ms submitted March 2004